Electronic Supplementary Material (ESI) for Journal of Materials Chemistry A.

Supporting Information

Performance improvement of MXene-based perovskite solar cells upon property transition from metallic to semiconductive by oxidation of $Ti_3C_2T_x$ in air

Lin Yang [a], Dongxiao Kan [a], Chunxiang Dall'Agnese [a], Yohan Dall'Agnese [b], Baoning Wang [a], Ajay Kumar Jena [c], Yingjin Wei [a], Gang Chen [a], Xiao-Feng Wang [a, *], Yury Gogotsi [d] and Tsutomu Miyasaka [c]

[a] *Key Laboratory of Physics and Technology for Advanced Batteries (Ministry of Education), College of Physics, Jilin University, 2699 Qianjin Street, Changchun 130012, China*

[b] *Institute for Materials Discovery, University College London, London WC1E 7JE, United Kingdom*

[c] *Graduate School of Engineering, Toin University of Yokohama, 1614 Kurogane-cho, Aoba, Yokohama, Kanagawa 225-8503, Japan*

[d] *A. J. Drexel Nanomaterials Institute, and Department of Materials Science and Engineering, Drexel University, Philadelphia, Pennsylvania 19104, United States*

Corresponding Authors

* Xiao-Feng Wang, *E-mail*: xf_wang@jlu.edu.cn

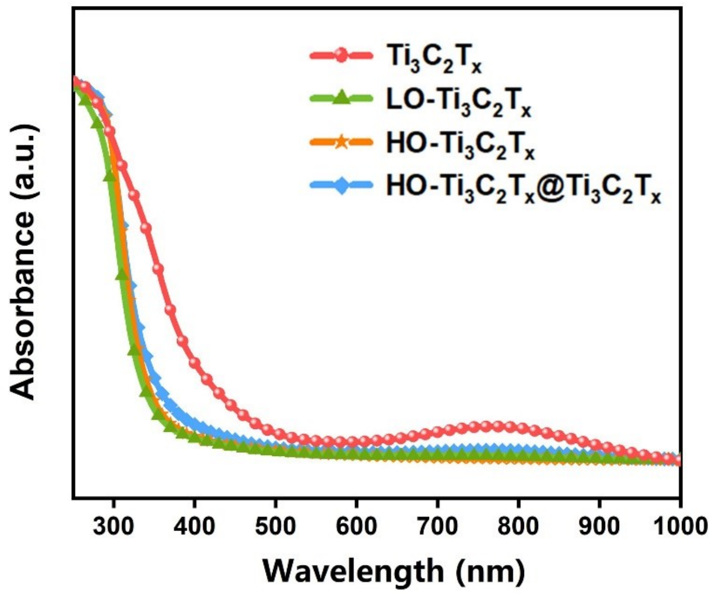

Figure S1. UV–vis absorption spectra of $Ti_3C_2T_x$, LO-$Ti_3C_2T_x$, HO-$Ti_3C_2T_x$ and HO-$Ti_3C_2T_x$@$Ti_3C_2T_x$.

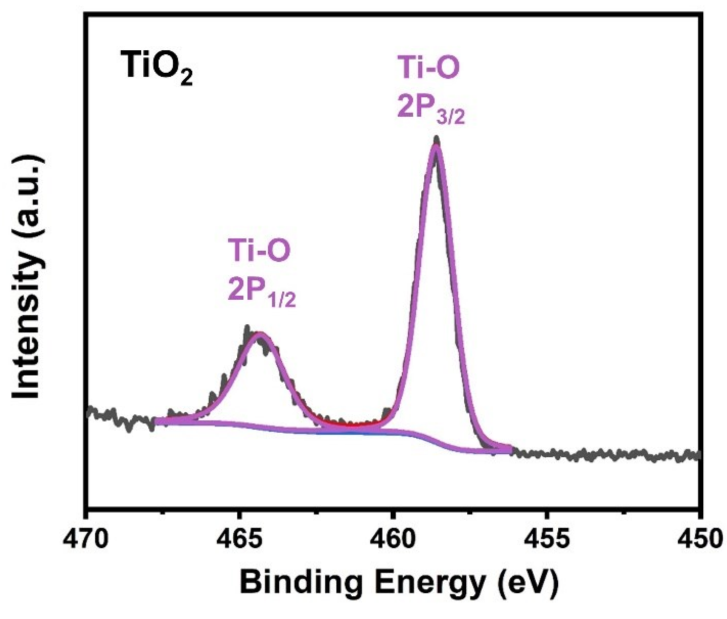

Figure S2. Ti 2p core level XPS spectra of the films of TiO_2.

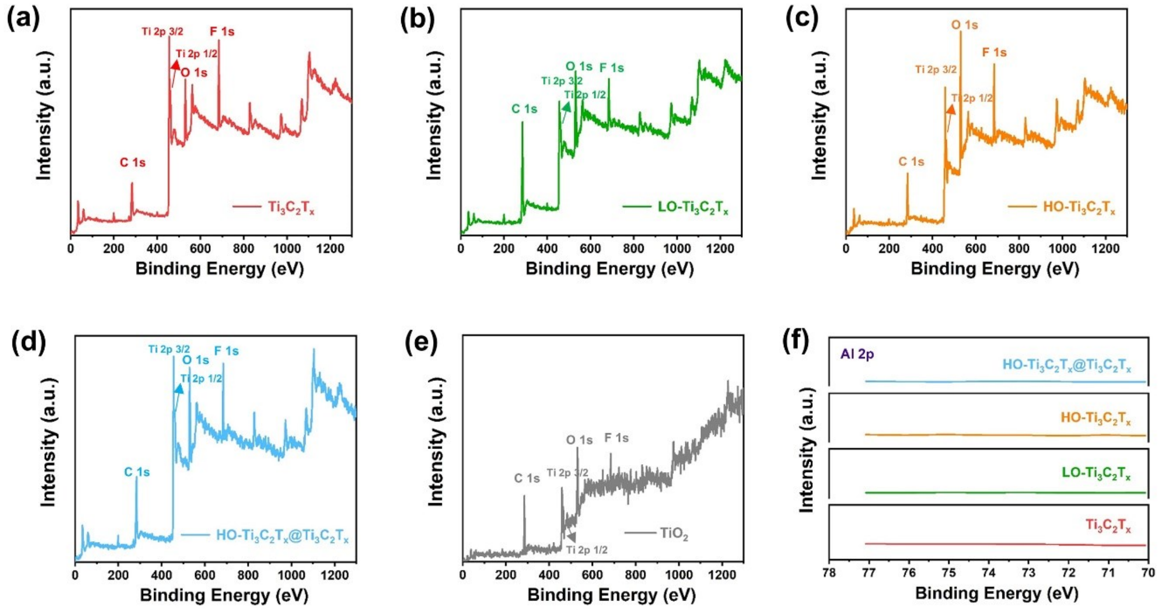

Figure S3. XPS spectra of the films of (a) $Ti_3C_2T_x$, (b) LO-$Ti_3C_2T_x$, (c) HO-$Ti_3C_2T_x$, (d) HO-$Ti_3C_2T_x$@$Ti_3C_2T_x$ and (e) TiO_2, respectively. (f) High resolution XPS spectra for Al 2p region for $Ti_3C_2T_x$, LO-$Ti_3C_2T_x$, HO-$Ti_3C_2T_x$ and HO-$Ti_3C_2T_x$@$Ti_3C_2T_x$.

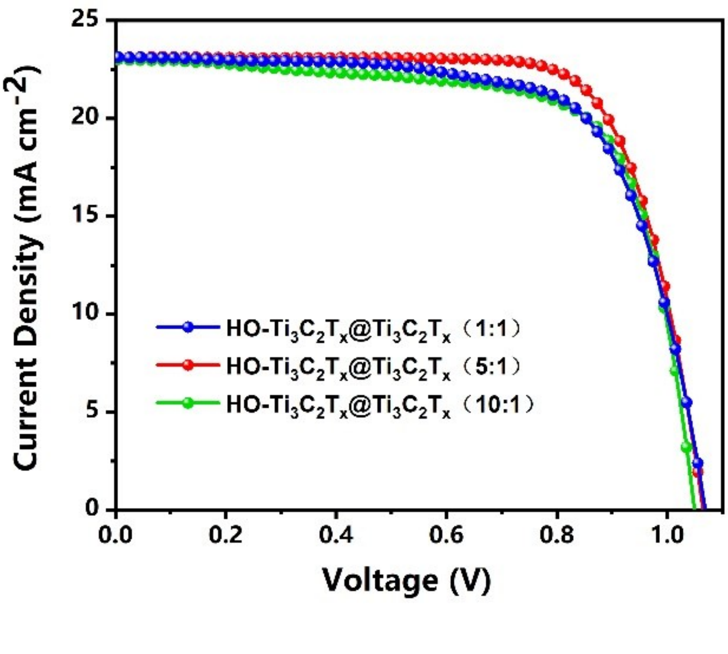

Figure S4. Reverse scan of PSCs' J–V curves based on HO-$Ti_3C_2T_x$@$Ti_3C_2T_x$ with different volume ratio (1:1, 5:1 and 10:1) as ETLs under AM 1.5 G simulated illumination.

Table S1. The photovoltaic performance parameters of PSCs with reverse scan based on HO-$Ti_3C_2T_x$@$Ti_3C_2T_x$ with different volume ratio of 1:1, 5:1 and 10:1 as ETLs under AM 1.5 G simulated illumination.

ETL	V_{oc}（V）	J_{sc}（mA cm^{-2}）	FF（%）	PCE（%）
HO-$Ti_3C_2T_x$@$Ti_3C_2T_x$ (1:1)	1.06	23.12	69	16.91
HO-$Ti_3C_2T_x$@$Ti_3C_2T_x$ (5:1)	1.07	23.11	74	18.29
HO-$Ti_3C_2T_x$@$Ti_3C_2T_x$ (10:1)	1.06	22.83	69	16.63

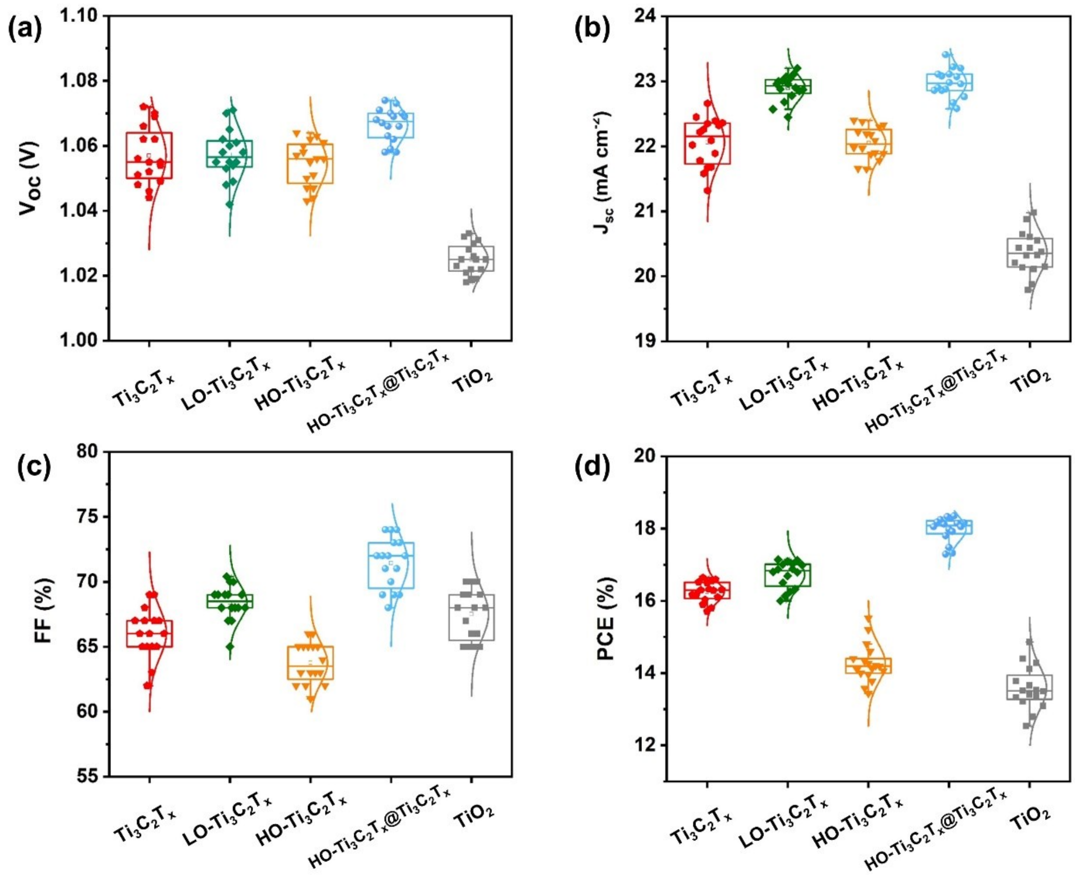

Figure S5. Photovoltaic parameter statistics of (a) V_{oc}, (b) J_{sc}, (c) FF and (d) PCE for the investigated PSCs. Parameters are extracted from the *J–V* curves acquired with reverse scan of 16 PSCs for each condition under AM 1.5 G simulated illumination.

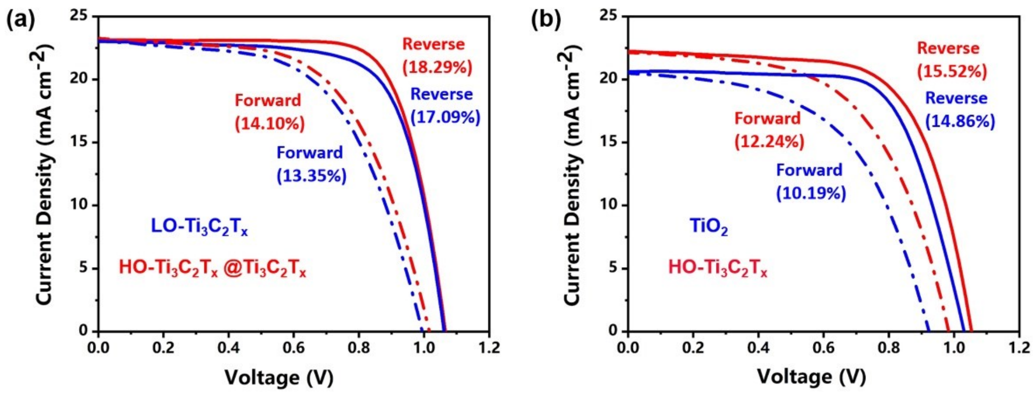

Figure S6. Forward and reverse scans of J–V curves for the devices based on (a) LO-$Ti_3C_2T_x$, HO-$Ti_3C_2T_x$@$Ti_3C_2T_x$ and (b) TiO_2, HO-$Ti_3C_2T_x$.

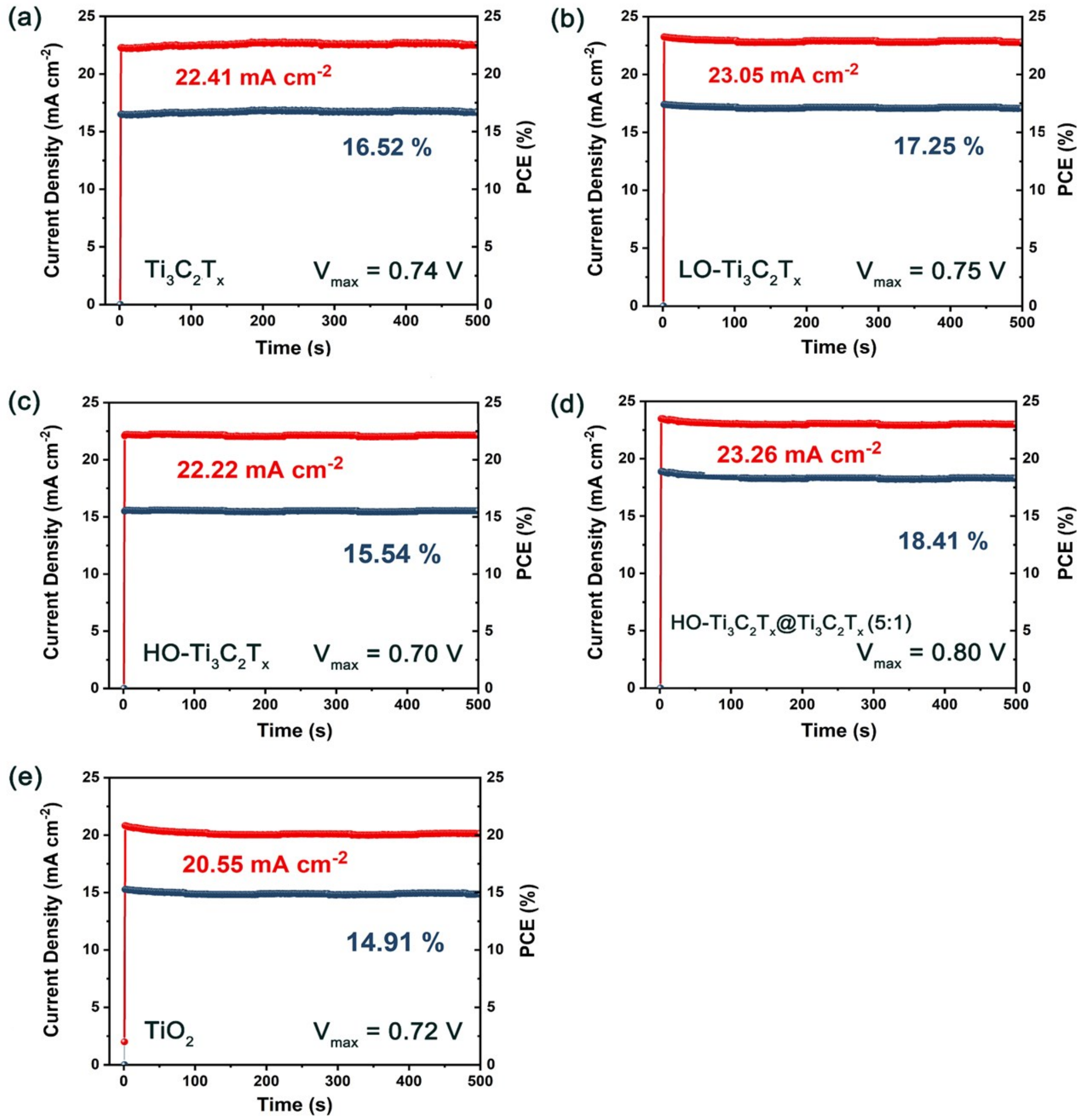

Figure S7. Steady-state power output and current density of devices based on (a) $Ti_3C_2T_x$, (b) LO-$Ti_3C_2T_x$, (c) HO-$Ti_3C_2T_x$, (d) HO-$Ti_3C_2T_x$@$Ti_3C_2T_x$ and (e) TiO_2 as ETLs, respectively.

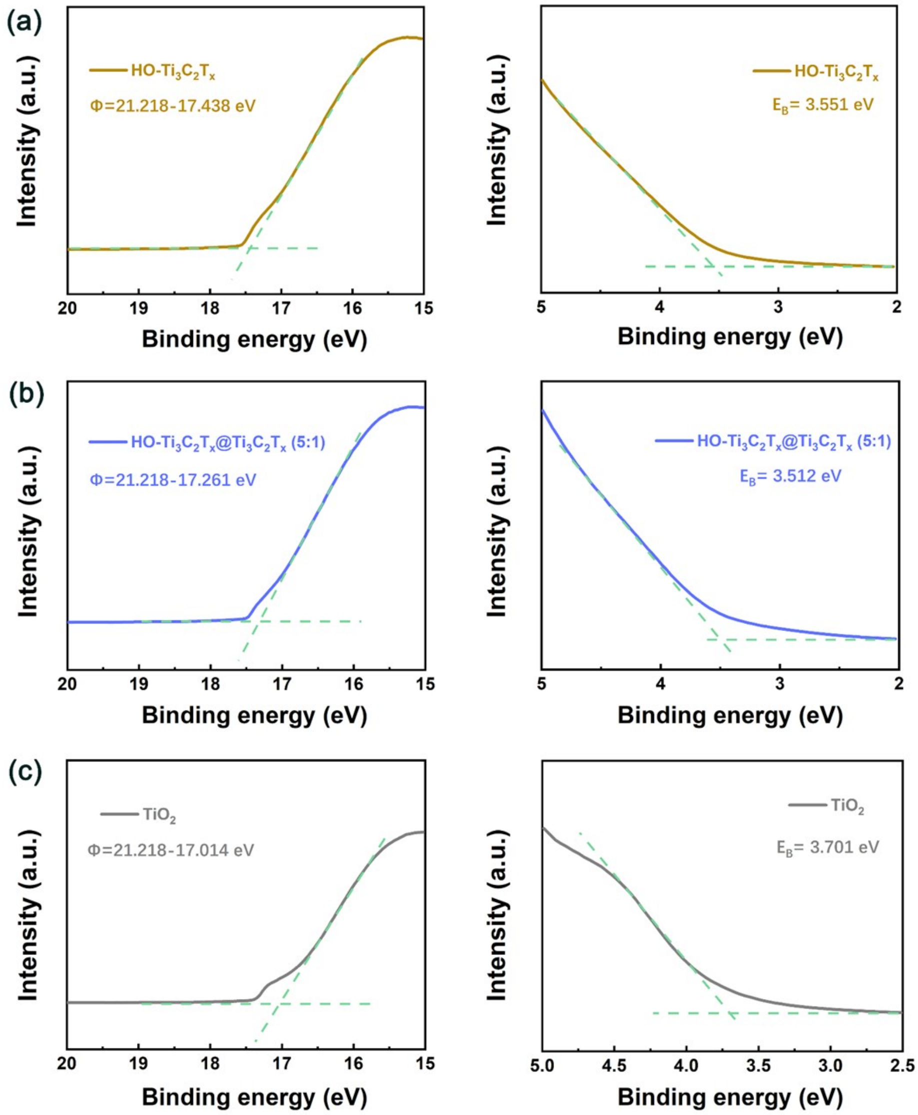

Figure S8. Ultraviolet photoelectron spectra of (a) HO-$Ti_3C_2T_x$, (b) HO-$Ti_3C_2T_x$@$Ti_3C_2T_x$ and (c) TiO_2 films spin-coated onto ITO substrates. The HOMO energy levels were determined by the intersection of baseline with the tangent line of the spectra, which is, HOMO = – (Φ + E_B) (eV).

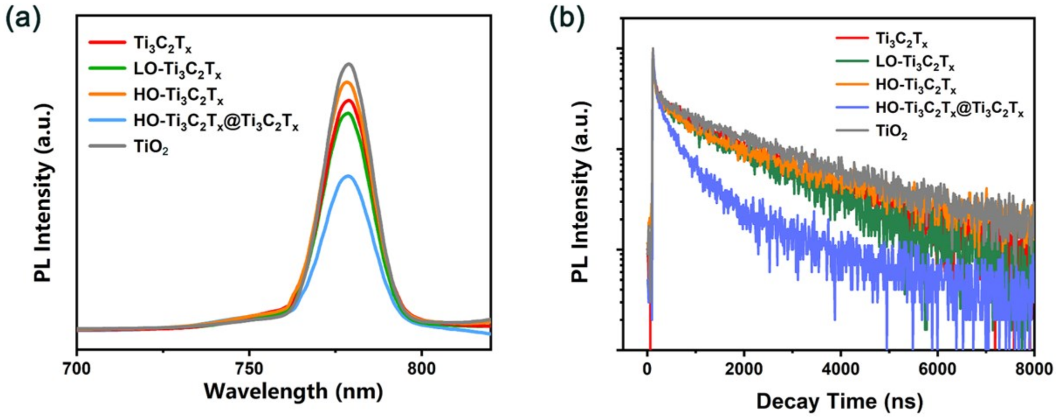

Figure S9. PL and TRPL spectra (excitation at 403 nm) of ITO/$Ti_3C_2T_x$/$CH_3NH_3PbI_3$, ITO/LO-$Ti_3C_2T_x$/$CH_3NH_3PbI_3$, ITO/HO-$Ti_3C_2T_x$/$CH_3NH_3PbI_3$, ITO/HO-$Ti_3C_2T_x$@$Ti_3C_2T_x$/$CH_3NH_3PbI_3$ and ITO/TiO_2/$CH_3NH_3PbI_3$.

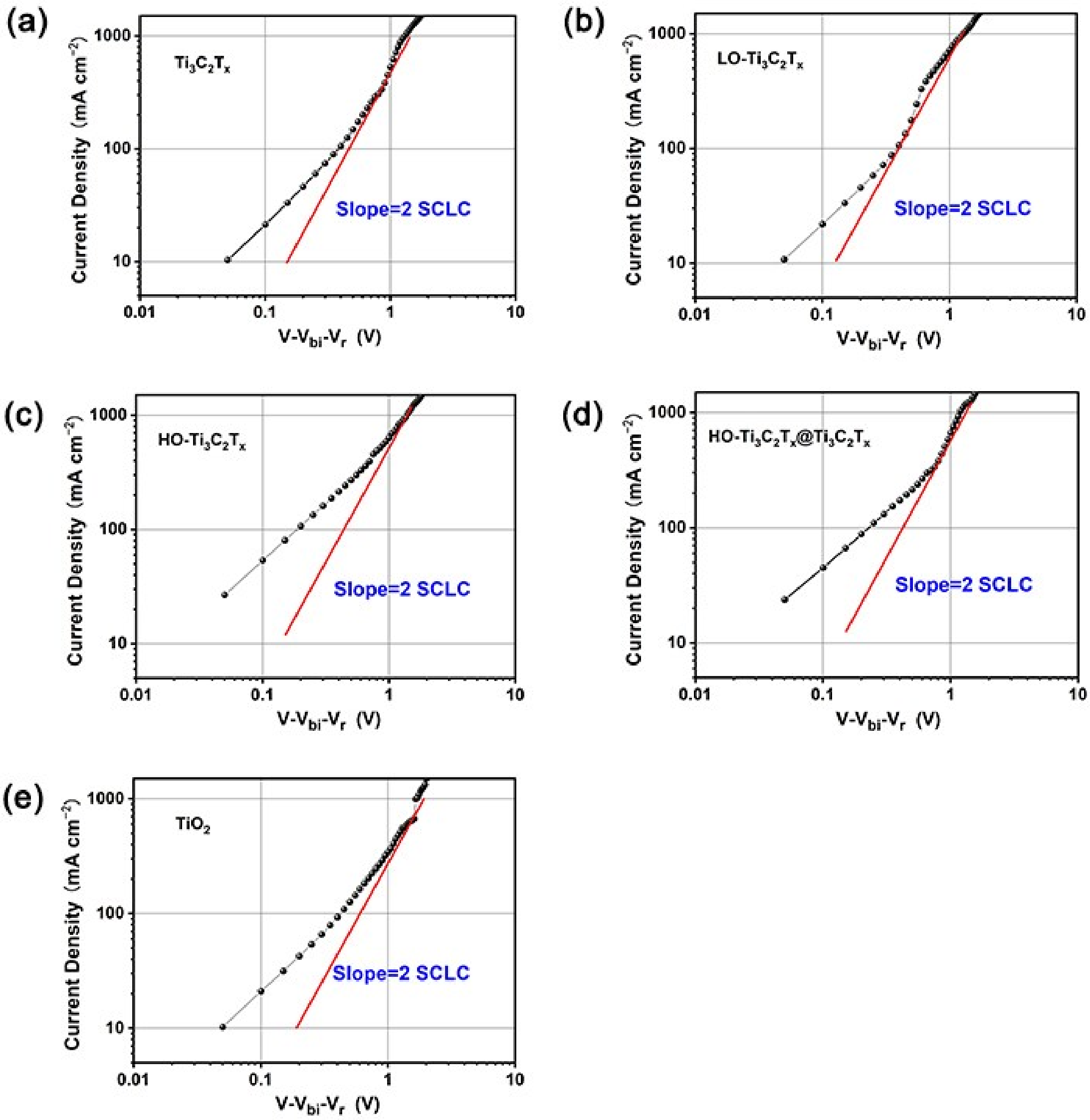

Figure S10. Typical *J–V* curves for the devices based on (a) $Ti_3C_2T_x$, (b) LO-$Ti_3C_2T_x$, (c) HO-$Ti_3C_2T_x$, (d) HO-$Ti_3C_2T_x$@$Ti_3C_2T_x$ and (e) TiO_2 as ETLs under dark, respectively.

The electron mobilities of ETLs were analyzed by the *J-V* curves with the electron-only structure of ITO/SnO_2/ETL/BCP/Ag under dark, and were calculated with the following equation:

$$J = 9\varepsilon_0\varepsilon_r\mu(V - V_{bi} - V_r)^2/8L^3$$

where μ is electron mobility ($cm^2\ V^{-1}\ s^{-1}$), J represents the current density ($mA\ cm^{-2}$), ε_0 indicates the permittivity of free space ($mA\ s\ V^{-1}\ cm^{-1}$), ε_r represents the dielectric constant of ETLs (assumed as 3), V is the applied voltage (V), V_r is the voltage drop (V) due to the series resistance and contact resistance across the electrodes, V_{bi} is the built-in voltage (V), $V-V_{bi}-V_r$ is obtained through a slope in the double log plot equals to 2, and L is the thickness of ETLs film (cm).

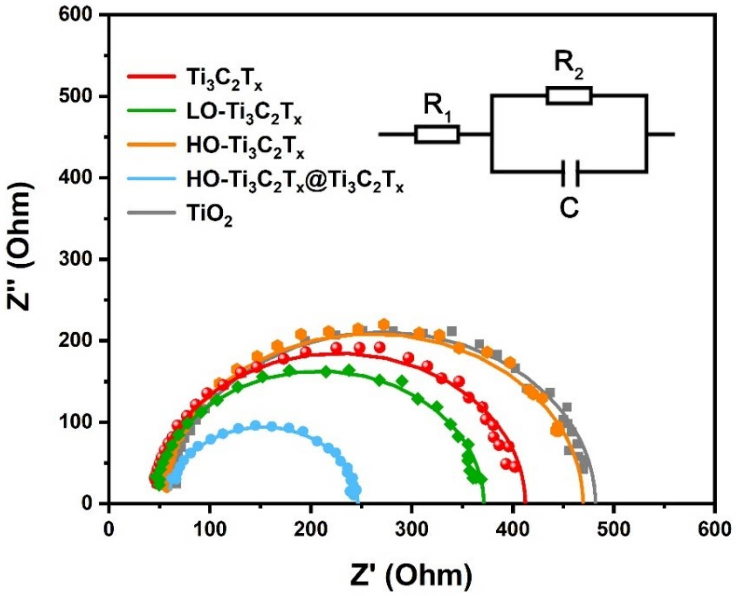

Figure S11. Nyquist plots of the PSCs based on $Ti_3C_2T_x$, LO-$Ti_3C_2T_x$, HO-$Ti_3C_2T_x$, HO-$Ti_3C_2T_x$@$Ti_3C_2T_x$ and TiO_2 as ETLs under one sun illumination, where the scattered points are experimental data and the solid lines are the fitted curves according to the equivalent circuit.

Table S2. Fitting parameters for EIS data.

ETL	R_1 (Ω)	R_2 (Ω)	C (F)
$Ti_3C_2T_x$	42.78	369.5	7.456E-9

LO-$Ti_3C_2T_x$	45.53	325.6	6.698 E-9
HO-$Ti_3C_2T_x$	51.96	417.5	7.429 E-9
HO-$Ti_3C_2T_x$@ $Ti_3C_2T_x$	56.28	188.2	8.394 E-9
TiO_2	59.73	422.1	6.921E-9

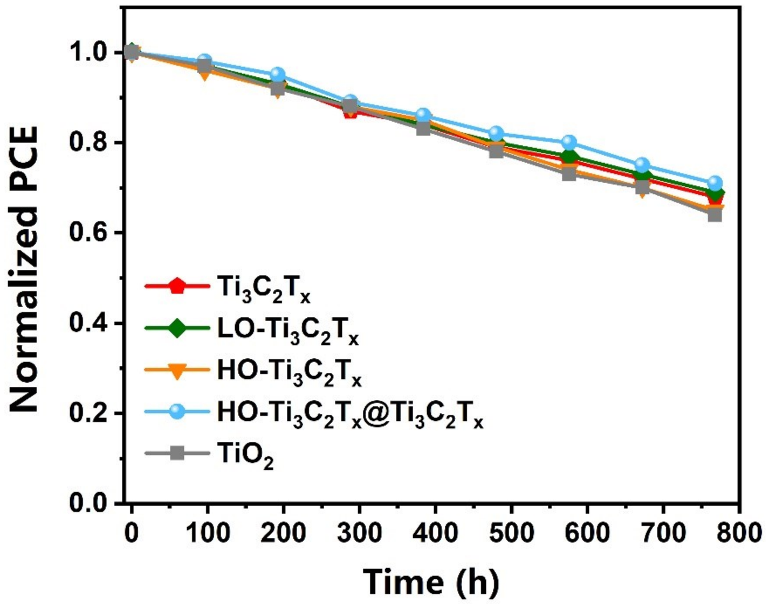

Figure S12. Stability results of PSCs based on $Ti_3C_2T_x$, LO-$Ti_3C_2T_x$, HO-$Ti_3C_2T_x$, HO-$Ti_3C_2T_x$@$Ti_3C_2T_x$ and TiO_2 as ETLs in ambient air (relative humidity ≈ 20%) without encapsulation at 25 °C.